Sustainable Food Technology

ROYAL SOCIETY OF CHEMISTRY

PAPER

View Article Online
View Journal | View Issue

Cite this: *Sustainable Food Technol.*, 2026, **4**, 2022

Valorization of onion peels into sustainable preservative films for enhanced food shelf-life

Neera Agarwal and Meena Krishania *

Plastic pollution, food wastage due to spoilage, and the underutilization of agricultural byproducts cause an increasing burden to the global food system. This study presents a solution to achieve a sustainable food technology by valorizing onion peels—an abundant agro-waste—into biodegradable, preservative-active packaging films. In this study, two distinct combinations of polymer matrices were developed: (i) 0.3% gellan gum and 0.3% xanthan gum (film G) and (ii) 0.3% guar gum and 0.5% sodium alginate (film O). These films, when blended with onion peel extract (OPE), showed potential to exhibit natural preservative properties. The detailed characterization of OPE-blended films was performed by FTIR spectroscopy, XRD, SEM, and TGA. OPE-blended films were more ductile and thermostable and had a higher UV resistance than the control films (without OPE), making them ideal for food storage. OPE exhibited a stronger antimicrobial activity than the commercial preservative sodium benzoate (SB), with lower MIC and MBC values against *E. coli*, *B. megaterium*, *S. aureus*, and *C. albicans*. Grapes coated with casting solutions of OPE-containing films G and O showed an extended shelf life up to 15 days at 25 °C, while blueberries packed in the OPE-blended films showed significantly reduced moisture loss. This innovation directly supports UN SDG 12 and UN SDG 8, ensuring sustainability and waste valorization. The novel combination of polymer matrices for sustainable food preservation shows immense potential in the food industry and the packaging sector.

Received 30th October 2025
Accepted 27th December 2025

DOI: 10.1039/d5fb00790a

rsc.li/susfoodtech

Sustainability spotlight

The global food system faces mounting challenges from plastic pollution, food spoilage, and underused agricultural by-products. This study offers a sustainable solution by valorizing onion peels—an abundant agro-waste—into biodegradable, preservative packaging films using novel combinations of xanthan gum, guar gum, gellan gum, and sodium alginate. These cost-effective, edible films exhibit enhanced antimicrobial, UV-resistant, and moisture-retentive properties, extending food shelf life while reducing synthetic plastic use. Aligned with UN SDGs 12 and 8, this innovation addresses consumer demands for eco-conscious materials, supports waste-to-resource strategies, and promotes circular economy principles, making it a viable path toward sustainable food preservation and green industry growth.

1. Introduction

An important aspect of food processing is food packaging. At present, many synthetic and natural materials are used as food packaging materials. However, the use of non-biodegradable synthetic materials could result in pollution, thus increasing the global carbon footprint.[1] Moreover, nowadays, consumers are more aware of their health and prefer the usage of environmentally sustainable materials for their daily needs, whether it be for clothing, food ingredients, or wrapping materials, which makes them more inclined towards sustainable, biodegradable, edible food packaging materials. Food packaging materials such as films can also be activated using a bioactive compound and thus used as a preservative. Wrapping materials could also be in the form of films, which are made using different biopolymers. To be effective as a preservative, the packaging film should confer antimicrobial activity, prevent moisture loss, and reduce oxidation of the food. Moreover, as the films are biodegradable, they would help in maintaining a safe environment and lead us towards a healthy future. Some polysaccharide-based films have an inherent antimicrobial activity, but for those that do not, this property could be rendered by adding certain bioactive compounds.[2] These bioactive compounds would not only reduce the microbial contamination of foods but also enhance the overall quality of food products, thereby increasing their shelf life. Among polysaccharides, chitosan, starch, cellulose, alginate, and pectin are widely used for the preparation of edible films. Xanthan gum and guar gum are another set of cheap and vegan polysaccharide gums, which can be used for film preparation. These gums usually have weak or no antimicrobial activity. Hence, a bioactive agent should be added to these matrices to make films with a preservative effect.

BRIC-National Agri Food and Biomanufacturing Institute (Formerly CIAB), Sector-81, Mohali, 140306, India. E-mail: meena@ciab.res.in

Onion is widely used around the world in different culinary practices, which results in a large amount of waste generation. Onion waste generally includes onion peels, which are removed either before sale or during cooking. Although these peels are rich in flavonoids, onion peel waste is also undesirable for landfills and composting due to its undesirable odor. Onion peel extract exhibits antimicrobial activity towards a vast range of microorganisms.[3] The OPE also possesses antioxidant, anti-obesity, antidiabetic, anticancer, and anti-inflammatory properties.[4] Hence, a novel and sustainable method of using these flavonoid-rich wastes should be explored. Therefore, we sustainably used onion peels to produce antimicrobial films, along with different polysaccharides like xanthan gum, guar gum, gellan gum, and sodium alginate.

Xanthan gum is a branched polysaccharide composed of repeating pentasaccharides. Each pentasaccharide unit is composed of two D-glucose units, two D-mannose units, and one D-glucuronic acid unit.[5] Xanthan gum can absorb a large amount of water and is used as a thickener and stabilizer. Its property of changing viscosity with temperature makes it desirable in food industries.[6] In pharmaceutical industries, it is used in various drug delivery formulations.[7] Guar gum is derived from a native plant of India and Pakistan, *Cyamopsis tetragonolobus*. It is a polymer composed of 2 units of mannose with one unit of galactose. In food industries, it is used as a stabilizer and thickener.[8] Similar to xanthan gum, it can swell up in water to form a viscous solution. Guar gum has also proven to lower cholesterol levels in the blood.[9] Gellan gum is an anionic exopolysaccharide consisting of repeating tetrasaccharide units containing two units of D-glucose, one unit of D-glucuronic acid, and one unit of L-rhamnose.[10] It is naturally produced through submerged fermentation of *Sphingomonas elodea*.[1] In food industries, it is used as an emulsifier, thickener, and stabilizer. It is also known to show high thermostability and pH stability. Sodium alginate is another naturally occurring polysaccharide, and contains β-D-mannuronic acid and α-L-guluronic acid as monomers. It is extracted from brown algae or kelp. It is a low-cost biodegradable polymer, extensively used in

Table 1 Overview of various onion peel extract-based film systems

OPE used (dry/liquid extract)	Film matrix/polymer system	Application	Reference
Liquid onion extract	Sodium alginate	Antioxidant/antimicrobial films	Santos *et al.* 2021 (ref. 13)
Liquid onion extract	Methylcellulose films	pH-sensitive antioxidant films	Gulati *et al.* 2023 (ref. 14)
Dry onion extract incorporated into plastics	Low-density polyethylene (LDPE)	Active packaging for shelf-life extension of chicken thigh	Moradi *et al.* 2023 (ref. 15)
Dry onion extract of yellow onion peels	Funoran	Active biodegradable films with antioxidant activities	Ju & Song, 2020 (ref. 16)
Liquid onion extract	Silver nitrate, and polyvinyl alcohol (PVA)	Antimicrobial films	Puišo *et al.* 2024 (ref. 17)
Dry onion powder	Karaya/Artemisia sphaerocephala Krasch. gum	pH-sensitive NH_3 responsive films	Liang *et al.* 2018 (ref. 18)
Liquid onion extract	Gelatin and sodium alginate	Milk freshness indicator, intelligent packaging films	Devi *et al.* 2024 (ref. 19)
Liquid onion extract	Gelatin	Shelf-life extension of rainbow trout fillets	Uçak *et al.* 2019 (ref. 20)
Dry onion extract and liquid extract	Carboxymethyl cellulose (CMC) and boron nitride nanoparticles	Antioxidant and biodegradable films	Pirsa *et al.* 2024 (ref. 21)
Dry powder of onion peel extract and onion stalk extract	Gluten/CMC/sodium alginate blends	Shelf-life extension of freshly peeled shallot onions	Thivya *et al.* 2022 (ref. 22)
Liquid onion extract	Corn starch/κ-carrageenan	Antimicrobial, biodegradable films	Wang *et al.* 2022 (ref. 23)
Dried onion extract	Chitosan	Shelf-life extension of lard, antimicrobial packaging films	Wang *et al.* 2022 (ref. 55)
Liquid onion extract	Chitosan/cinnamon essential oil/gum arabic	Antimicrobial, antioxidant films	Rajendran *et al.* 2024 (ref. 24)
Cyanidin-rich dried extract (OE) anchored on a halloysite-layered double hydroxide filler.	Potato starch/halloysite nanotubes	pH-sensitive nanocomposite films	Boccalon *et al.* 2022 (ref. 25)
Liquid onion extract	Cellulose acetate	Antioxidant, biodegradable films	De Dicastillo *et al.* 2015 (ref. 26)
Dried onion extract	PVA–cellulose nanocrystals (CNC)	Antimicrobial, packaging films	Hamid Salim *et al.* 2025 (ref. 27)
Liquid onion extract	Polyethylene terephthalate (PET)	Antioxidant PET-based packaging	Idris & Othman, 2023 (ref. 28)
Dried onion extract	(i) Gellan gum/xanthan gum	(i) Extended shelf life of grapes coated with OPE-containing film casting solution	This study
	(ii) Sodium alginate and guar gum	(ii) Moisture retention of blueberries when packed in OPE-blended films (iii) Antioxidant, antimicrobial active OPE- blended films	

food industries as a thickener, stabilizer, and gelling agent.[11] A precise drug delivery system and injectable implants for bone or cartilage regeneration could be developed using sodium alginate.[12]

Previously, many studies have demonstrated the use of onion peels to activate edible polysaccharide films (Table 1). These include sodium alginate,[13] methylcellulose films,[14] low-density polyethylene or LDPE films,[15] funoran,[16] gelatin-silver nitrate matrix,[17] Artemisia sphaerocephala Krasch. gum,[18] gelatin,[19,20] carboxy methyl cellulose (CMC),[21] gluten/CMC/sodium alginate,[22] corn starch/κ-carrageenan,[23] chitosan,[24] potato starch/halloysite nanotubes,[25] cellulose,[26] polyvinyl alcohol (PVA)-cellulose nanocrystals (CNCs),[27] and polyethylene terephthalate.[28] The solvent used to extract the bioactive compounds should be carefully selected, as it should be able to efficiently dissolve the desired antioxidant and antimicrobial compounds, which need to be extracted.[29] For the preparation of edible films, a single polymer or a blend of different polymers could be used. This can enhance the cost-performance ratio, mechanical properties, and stability of the resulting product.[30,31]

In the present work, a novel combination of xanthan gum/guar gum/gellan gum and xanthan gum/guar gum/sodium alginate has been explored. This combination of polymer matrices has not been previously reported for film fabrication. Moreover, to the best of our knowledge, OPE has never been incorporated into films composed of gellan gum/xanthan gum or sodium alginate/guar gum. These polysaccharides are cost-effective and readily available. Thus, the article demonstrates the preparation and characterization of the unique films composed of two different polysaccharide combinations: xanthan gum-gellan gum and guar gum-sodium alginate, activated using OPE powder. Their physical, optical, and mechanical properties were studied and compared with the blank films (with no OPE), which has not been previously reported for these polymer combinations. Further, the antibacterial properties of the OPE-blended films were studied, and their use as preservatives was analyzed on grapes and blueberries to assess their commercial applicability.

This innovation directly supports UN SDG 12: Responsible Consumption and Production by transforming food waste into value-added materials, reducing plastic use, and minimizing spoilage. It also aligns with UN SDG 8: decent work and economic growth by encouraging eco-innovation and creating sustainable job opportunities in food packaging and waste valorization sectors. Hence, it addresses consumer demands for eco-conscious materials, supports waste-to-resource strategies, and promotes circular economy principles, making it a viable path towards sustainable food preservation and green industry growth.

2. Materials and methods

2.1. Chemicals

Xanthan gum and Guar gum were procured from Central Drug House (P) Ltd (India). The chemicals sodium alginate, gellan gum, glycerol, and sodium benzoate were purchased from Sigma-Aldrich. Onion peels were procured from a local vegetable vendor.

2.2. Preparation of composite films

The composite films (A–R) were prepared in different proportions, as described in Table S1.

A total of 50 mL solution for individual films A–E was prepared by dissolving 0.3% XG/0.3% GuG in water using a handheld homogenizer at room temperature (25 °C). The solution was then heated and stirred at 55 °C for 90 minutes to obtain a homogeneous solution. Then, 40% glycerol, a plasticizer, was added to the mixture, and the mixture was heated again at 55 °C for 30 min. The prepared solution was then cast onto a 90 mm Petri plate. For the preparation of films G–Q, two different polymer solutions were prepared. Solution I, containing 0.3% gellan gum, was dissolved in water at 55 °C for 30 min. Meanwhile, at room temperature (25 °C), solution II(a) was prepared by dispersing 0.3% xanthan gum (for films G, I, and K) and solution II(b) 0.3% guar gum (for films M, O, and Q) in water using a handheld homogenizer. Then, solution II(a or b) was added to solution I for the preparation of the respective polysaccharide blend (for films G, I, and K or M, O, and Q). The resulting prepared mixtures were then stirred at 55 °C for 90 min using a magnetic stirrer to ensure homogeneity. Then, 40% (w/w) glycerol was added to the respective mixtures. The mixtures were again stirred for 30 min. The homogeneous film-forming mixtures were then cast onto a 90 mm Petri plate individually. The films were dried in a hot-air oven at 50 °C overnight. The films were taken out the next day and stored at 40% relative humidity (RH).

A similar procedure was used to prepare sodium alginate/xanthan gum/guar gum amalgam films (L–Q). All the films were stored at 25 °C and 40% RH for at least 48 h before proceeding to their characterization.

2.2.1. Preparation of OPE-blended films. For the preparation of OPE-blended films, lyophilized OPE powder (w/w) was added to the film-forming solution after the addition of glycerol and stirred for 10 minutes to obtain a homogeneous solution. The solution was then cast onto a Petri plate. Different amounts of OPE, 1%, 5%, 10%, 15% and 20% (w/w), were added into the solution to prepare OPE-blended films. All the films were coded according to the OPE concentration. For example, for film G, the films were coded as G1 (containing 1% OPE), G5 (containing 5% OPE), G10 (containing 10% OPE), G15 (containing 15% OPE), and G20 (containing 20% OPE).

2.3. Preparation of onion peel extract (OPE)

To prepare OPE, onion peels were first thoroughly washed with water and dried in an oven at 50 °C. The peels were then crushed using a mixer grinder to obtain a fine powder. The onion peel powder (3 g) was placed in a thimble, and the extraction of bioactive compounds was performed using a solvent extractor (VELP Scientifica) with 70 mL of 80% ethanol. The extraction was done at 60 °C for 90 minutes. Ethanol was chosen as it can extract the required bioactive compounds, and is safe and economical.[32] The OPE produced was then lyophilized to obtain a powdered mass. The OPE dried powder was stored at 4 °C until further use.

2.3.1. Determination of the total phenolic content (TPC). The TPC of onion peel extract (powdered) and OPE-blended

films was determined using the Folin-Ciocalteu colorimetric method, as described by Narnoliya *et al.* 2019,[33] with slight modifications. A 400 μL sample was mixed with 200 μL FC reagent (10-fold diluted) and incubated for 10 min in the dark. After the incubation, 100 μL 7.5% Na_2CO_3 was added to the reaction mixture and incubated again in the dark for 25 min. The volume was made up to 1 mL using water. The absorbance was measured at 765 nm using a spectrophotometer. Here, gallic acid was used as the standard for TPC estimation (Fig. S2). The TPC value was calculated in mg GAE per g.

For OPE-blended films, about 100 mg of film was cut and immersed in 10 mL of distilled water for 24 h. Undissolved films were removed by centrifugation, and the solution was then used for TPC calculation using the above method. The procedure for TPC determination in films was similar to that reported by Wang *et al.* 2022.[23]

2.3.2. Determination of the antioxidant activity of OPE. The antioxidant activity of OPE was determined using DPPH (α,α-diphenyl-β-picrylhydrazyl) by a method described by Hu *et al.* 2014,[34] with slight modifications. Briefly, a 0.1 mM DPPH-methanol solution (Met-DPPH) was used for determining the radical scavenging activity. First, 1 mL sample was mixed with 1 mL of 0.1 mM Met-DPPH. The mixture was incubated for 30 min in the dark, and the absorbance was measured at 517 nm. The mixture with only solvent (methanol) and DPPH was taken as a blank. The DPPH scavenging activity was determined using eqn (1):

$$[(OD_{517}\ \text{control} - OD_{517}\ \text{sample})/OD_{517}\ \text{control}] \times 100 \quad (1)$$

To determine the IC_{50} value of OPE, the radical scavenging activity at different concentrations of OPE was determined. The OPE concentration at which a 50% reduction of DPPH was observed was determined to be the IC_{50} value.

2.4. Characterization of the composite films

2.4.1. Visual characterization and thickness of films. The films were visually characterized for their color, odor, flexibility, and texture. The thickness of the films was determined using vernier calipers. The thickness of 5 random positions on the film was determined, and the average value was considered the actual film thickness.

2.4.2. Scanning electron microscopy. SEM (SEM, JEOL, JSM-IT300) was performed to study the surface morphology of the films (with and without OPE). Before the SEM imaging, the samples were prepared by gold sputtering in a low-vacuum chamber at an accelerating voltage of 10 kV.

2.4.3. Moisture content of films. The moisture content of films is an important attribute to be considered while using edible films. To determine the water content of the films prepared, a known amount of each film (W_i) was weighed and incubated in a hot-air oven at 105 °C. The final weight of the films was recorded after 24 h (W_f). The moisture content was determined using eqn (2):

$$\text{Moisture content}\ \% = (W_i - W_f)/W_i \times 100 \quad (2)$$

where, W_i: weight of the film before incubation. W_f: weight of the film after incubation at 105 °C.

All the experiments were conducted in triplicate to ensure accuracy.

2.4.4. Solubility. To determine the solubility of films in water, a known amount of film was weighed and immersed in water at 25 °C for 24 h. The samples were manually shaken in between. The insoluble part was collected by centrifugation and dried in a hot-air oven at 50 °C. The dried film was weighed, and the solubility was calculated using eqn (3):

$$\text{Solubility}\ (\%) = [(W_i - W_0) - (W_f - W_0)]/(W_i - W_0) \times 100 \quad (3)$$

where, W_0: weight of the empty micro centrifuge tube (MCT). W_i: initial weight of the film + MCT. W_f: final weight of the dried insoluble film + MCT.

All the experiments were conducted in triplicate to ensure accuracy.

2.4.5. Swelling index of films. To determine the swelling index of the films, the method described by Galus & Kadzińska, 2016 (ref. 35) was used. The films were cut into equal sizes and weighed. The films were then dipped in distilled water for 2 min and gently blotted with filter paper to remove excess water. The swollen film was weighed again. The experiment was conducted at room temperature. The swelling index was calculated using eqn (4):

$$\text{Swelling index} = (W_f - W_i)/W_i \quad (4)$$

where, W_i: initial weight of films (mg). W_f: final weight of the swollen film (mg).

2.4.6. Opacity and transparency of films. The optical properties of the films were determined using a spectrophotometer, using the method described by Gasti *et al.* 2023.[36] The films were cut into strips (3 × 0.5 cm^2) and were inserted into a cuvette. The absorbance spectra of the films were recorded in the range of 200–800 nm using an empty cuvette (air) as a reference. The opacity and transparency of films were calculated using eqn (5) and (6), respectively:[37]

$$\text{Opacity of films} = (\text{absorbance of film at 600 nm})/(\text{film thickness (mm)}) \quad (5)$$

$$\text{Transparency of films}\ (\%T) = \text{transmittance}\ (\%) = 10^{(2\ -\ \text{absorbance})} \quad (6)$$

To check the effect of OPE incorporation on the spectral properties of the films, the transparency of the films (G and O) containing different OPE concentrations was also determined.

2.4.7. Fourier transform infrared (FT-IR) analysis of the prepared films. Fourier transform infrared spectra of the films and their constituents were recorded at room temperature using an FT-IR spectrometer (IR Spirit-X, Shimadzu, Kyoto, Japan). The spectra for each sample were recorded in the wavelength range of 450–4500 cm^{-1} spectral region.

To verify the incorporation of OPE into the films (G and O), the FTIR spectra of films with 1% OPE and 20% OPE were compared with that of the blank films.

2.4.8. Thermal gravimetric analysis (TGA) of the prepared films. Thermostability is an important aspect to be analyzed if the films have to be used at a higher temperature. To determine the thermal stability of the films, thermal gravimetric analysis (TGA) was performed using a PerkinElmer STA 8000 Simultaneous Thermal Analyzer. The thermograms were recorded from 30 °C to 800 °C at a heating rate of 15 °C min^{-1}, and the percentage of weight loss was measured at different temperatures.

To check the effect of OPE incorporation into the films (G and O), the thermal stability of 1% OPE- and 20% OPE-blended films was compared with that of the blank films.

2.4.9. Mechanical properties of films. The thickness of all the films was measured at five different locations using digital vernier calipers, and the average thickness was used for the calculation of their mechanical properties. The tensile strength (TS), Young's modulus (YM), and elongation at break (EAB) for films with and without OPE were determined at room temperature using a Universal Testing Machine (Shimadzu). Films were cut into rectangular strips with a width of 20 mm, and the TS was determined at a crosshead speed of 5 mm min^{-1}. The TS, YM, and EAB were calculated using eqn (7), (8) and (9), respectively:

$$\text{Tensile strength (TS)} = F/(w \times d) \quad (7)$$

where, F: maximum force applied on the film (N). w: width of the film (mm). d: film thickness (mm).

$$\text{Young's modulus (YM)} = \text{stress/strain} \quad (8)$$

$$\text{Elongation at break (EAB)} = (L_f - L_i)/L_i \times 100 \quad (9)$$

where, L_i: length of the film before elongation (mm). L_f: final length of the film after elongation (mm).

2.4.10. X-ray diffraction (XRD) analysis. The crystallinity or amorphous nature of the OPE-blended and blank films was checked by XRD analysis. The analysis was performed using a Rigaku SmartLab SE X-ray diffractometer at 40 kV and 30 mA. Cu-Kα radiation (λ = 1.54056 Å) was used for film characterization, and the 2θ range was measured in the range of 10° to 60°, with a scan speed of 2° min^{-1}. The results were analyzed using the Smart Lab Studio II software.

2.5. Antimicrobial activity of OPE-incorporated films

The antimicrobial properties of the OPE-blended films were checked using the agar diffusion test. The films with different concentrations of OPE were cut into 5 mm-diameter discs. The films' antimicrobial activity was tested against three bacteria, *Escherichia coli*, *Staphylococcus aureus*, and *Bacillus megaterium*, and a fungus, *Candida albicans*. For this, 100 μL of the respective bacterial culture with an optical density corresponding to 0.5 McFarland was spread on the nutrient agar plate (for bacteria) and on Yeast Extract Peptone Glycerol (YEPG) media (for fungus). Then, the film discs were placed on the surface of the agar plate and incubated at 30 °C for 18 hours. The plates were then checked for the presence of a zone of inhibition around the antimicrobial discs.

2.6. Determination of the MIC and MBC of OPE

The MIC and MBC of OPE against *E. coli*, *B. megaterium*, *S. aureus*, *and C. albicans* were compared to those of a readily used food preservative, sodium benzoate (SB). The MIC of SB was calculated using both the broth dilution method and the agar dilution method, whereas the MIC of OPE was determined solely by the agar dilution method. This was done because OPE, being dark purple/maroon colored, hindered the exact determination of MIC, as the growth of microbes could not be visually observed.[38] This was validated by determining the MIC of sodium benzoate using the agar dilution method.

For broth dilution, a EUCAST reference method described by Schön *et al.* 2020 (ref. 39) was used with slight modifications. Different concentrations of SB (total volume, 200 μL) were prepared in a 96-well plate. To this, 100 μL of microbial cell suspension (1 : 100 dilution of 0.5 McFarland equivalent) was added. The plate was incubated for 18 h at 32 °C. Positive control (with sterile broth and cells) and negative control (sterile broth only) were also prepared. The MIC was determined by visualizing the turbidity in the wells; the minimum concentration of SB at which microbial growth inhibition was observed was considered to be the MIC concentration.

For the agar dilution method, nutrient agar plates (for bacteria) and YEPG agar plates (for fungus) with different concentrations of SB and OPE were prepared. This was done by adding varying desired concentrations of antimicrobial agents after the temperature of the autoclaved agar reached ~45 °C. Then, 1 μL of a 1 : 10 diluted microbial sample (prepared from a 0.5 McFarland-adjusted bacterial culture) was spotted on agar plates with different antimicrobial concentrations. The plates were incubated at 32 °C for 18–24 h. The concentration of OPE and SB at which the microbial growth was inhibited was considered as the MIC value against the respective microbe.

The MBC was determined by subculturing the samples showing MIC (broth dilution method) on fresh agar plates. The growth of the microbes was observed after 18–24 h of incubation at 32 °C. The concentration of the antimicrobial agent at which the colony count decreased by 99.9% was considered the MBC for the organism.[40]

2.7. Preservative effect of OPE films

The preservative effect of OPE was checked and compared to a widely used food preservative, sodium benzoate. Equal concentrations of both OPE and sodium benzoate were used, and their antimicrobial activities were studied against different microbes, namely *E. coli*, *B. megaterium*, *S. aureus*, and an opportunistic pathogenic fungus, *Candida albicans*. The presence of a zone of inhibition depicted the antimicrobial activity of the two compounds. The zone of inhibition of OPE was compared to that of sodium benzoate after 18 h of incubation at 30 °C.

2.7.1. Fruit coating. To further validate the preservative effect of OPE, the film casting solutions of G and O containing 1% and 20% OPE were coated on a perishable fruit, grapes. Grapes are highly prone to spoilage if not stored properly, which results in their shorter shelf life. Attempts were made to increase the shelf life of grapes by dipping them in the prepared preservative coating. Two sets of grapes were made—one was stored at room temperature (25 °C) and the other set was stored at 4 °C. The grapes were checked for any spoilage/shrinkage after a few days of storage.

2.7.2. Packaging of blueberries. An alternative method to preserve perishable fruits is packing them in bags prepared using the developed films. Blueberries, another perishable fruit, were weighed and packed in the bags prepared from films containing 1%, 10% and 20% OPE and stored at two different temperatures, 25 °C and 4 °C. Packaging of the fruit in films was done using a heat sealer. After 15 days of incubation, the weight loss of the blueberries was recorded.

2.8. Statistical analysis

All the experiments were conducted in triplicate, and the mean values with standard deviation are presented in the tables and figures. The statistical tests were performed using the software Minitab® 20. Significant difference was determined by ANOVA (analysis of variance) and SPSS at 95% confidence value ($p \leq 0.05$), followed by Tukey's post hoc test.

3. Results and discussion

The preparation of edible films from various bioproducts has been reported previously. A gelling agent and a plasticizer are the basic requirements for the preparation of an edible film. In the present study, hydrocolloids like xanthan gum and guar gum were used with gelling agents, namely gellan gum and sodium alginate, to form films. All four gums are edible, and are widely used as thickeners, stabilizers, and emulsifiers in various food products like sauces, dairy products, and desserts. Glycerol has been used as a plasticizer. A plasticizer decreases the polymers' glass transition temperature, hence making a film softer and more flexible. This ensures that films have a higher mechanical strength, thermal stability, and shelf life.[1] Carboxyl or ester groups of xanthan gum/guar gum form hydrogen bonds with hydroxyl groups of gellan gum to form a stable interconnected network in the film. A ratio of gellan gum and xanthan gum (7 : 3) has been reported for the film preparation using PEG-400 as a plasticizer.[41] GuG has several hydroxyl groups, which can interact with the negatively charged carboxyl groups of the anionic polysaccharides like XG and GeG. Therefore, films made using guar gum, xanthan gum, and gellan gum can further show a synergistic effect on the mechanical properties along with less stickiness.[42] Sodium alginate can also form intermolecular hydrogen bonds with xanthan/guar gum to form stable films.[43] These films were characterized for their physical characteristics, and their intermolecular interaction was validated by FT-IR spectroscopy, XRD, and TGA. The need of the hour is a hydrophobic film with lesser solubility and moisture, which could also be used as a preservative wrapping material for perishable fruits, vegetables, and sweets. Besides serving as a preservative, such a film could extend the shelf life while maintaining the nutritional quality of the food item.

3.1. Characterization of the physical properties of films

3.1.1. Physical appearance of the films. Different films were prepared using xanthan gum, guar gum, gellan gum, and sodium alginate at different concentrations and combinations, as described in Table 2. All the films were white, transparent, and odorless (Fig. S1). Films A–F (Table S1) were sticky and not stable outside the desiccator. Film G (with 0.3% XG and 0.3% GeG) and film I (with 0.3% GuG and 0.3% GeG) were stable at room temperature. Films M and O were prepared using 0.5% SA with 0.3% XG and 0.3% GuG, respectively. Film K (0.3% XG + 0.3% GuG + 0.3% GeG) and film Q (0.3% XG + 0.3% GuG + 0.5% SA) were thicker and firmer than the other films due to the presence of three polysaccharides, which increased the solid mass of the film composite. Films H, J, L, N, P, and R were not analyzed as they had the same physical appearance as their respective counterparts (G, I, K, M, O, and Q, respectively), which contained a lower amount of polysaccharides, making further analysis unnecessary and aiding in cost reduction. Gellan gum-based films, G and I, were stable outside the desiccator but not as transparent and flexible when stretched as sodium alginate-based films M and O. The films prepared using sodium alginate (M and O) were also glossier than the films prepared using gellan gum (G and I). Films K and Q were translucent, less sticky, sturdy, and less flexible when stretched.

SEM analysis of the films revealed a homogeneous, smooth, and uniform surface, without any micropores or cracks, indicating efficient intercalation and good compatibility of the polysaccharides with each other (Fig. 1 and S3). In general, gellan gum-based films showed layered edges, which could be

Table 2 Composition of the prepared films

Films	Xanthan gum % (w/v)	Guar gum % (w/v)	Gellan gum % (w/v)	Sodium alginate % (w/v)	Glycerol conc. % (w/w)
G	0.3	—	0.3	—	40
I	—	0.3	0.3	—	40
K	0.3	0.3	0.3	—	40
M	0.3	—	—	0.5	40
O	—	0.3	—	0.5	40
Q	0.3	0.3	—	0.5	40

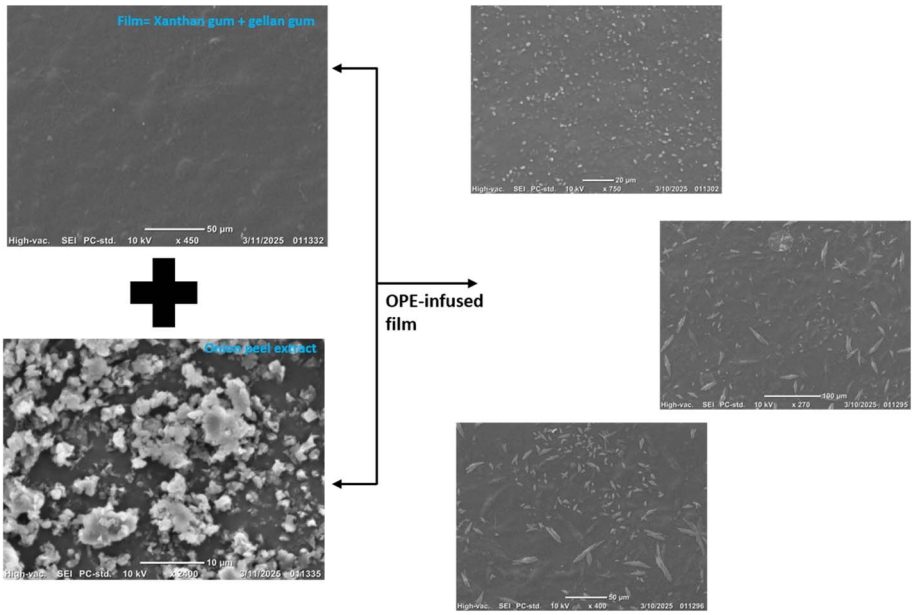

Fig. 1 SEM images showing blank film G (with xanthan gum and gellan gum), OPE, and OPE-blended film G.

due to the difference in polymer viscosity, which caused phase separation during the drying process (Fig. S3B). However, in alginate-based films, the edges are smoother and uniform, depicting better polymer compatibility and uniform flow behavior (Fig. S3A).

The determination of the thickness of films is important, as it affects the mechanical, optical, and physical properties of a film.[44] The thickness of the films was measured using digital vernier calipers with an error rate of 0.001 mm (Table 3). It was observed that the films prepared using sodium alginate (M and O) were thicker than those made with gellan gum (G and I). This could be because of the higher concentration of sodium alginate (0.5%) used than that of gellan gum (0.3%) for the film preparation. Moreover, the films prepared using three polysaccharides, namely K and Q, were significantly thicker ($p \leq 0.05$) than those prepared using two gums.

OPE-containing films were colored, and the color was directly proportional to the concentration of OPE added in the film-forming solution (Fig. S4). The thickness of the films significantly increased with the increase in the concentration of OPE (Table S2). This can be attributed to the increase in the total solid content and viscosity of the film-forming solution by the addition of OPE. Additionally, the moisture content in the films resulted in partial swelling and volumetric expansion, which can result in an increase in the film thickness. However, the thickness of film G with 20% OPE (0.06 mm) was significantly lesser ($p \leq 0.05$) than that of film O (0.085 mm) with 20% OPE. This could be due to the use of 0.5% SA in film O instead of 0.3% GeG in film G. Among the various film formulations (A–R), films G (GeG-based) and O (SA-based) were selected for subsequent blending with onion peel extract (OPE) and detailed characterization, as these matrices were stable and also represented the two optimal mechanical extremes—film G exhibiting the highest tensile strength and film O demonstrating the greatest flexibility (Section 3.7).

3.1.2. Moisture content, swelling, and solubility of films. Moisture content, or the amount of water present in the films, defines the applications of films. Water, which acts as a plasticizer, influences polymer chain mobility, free volume, and, consequently, the mechanical properties of a film.[45] If a film has a higher moisture content, it is highly prone to microbial growth, but is more flexible and ductile. This can result in the spoilage of the food, which is wrapped in the film, hence reducing its shelf life. Additionally, a low moisture film has an excellent water vapor barrier and improved mechanical properties. However, the film with low moisture confers a low-oxygen barrier, reduced flexibility, and poor adhesion due to restricted polymer chain mobility.[46] For an environmentally friendly

Table 3 Physical characteristics of the films. Means sharing different letters within a column indicate a significant difference ($p < 0.05$)

Film	Thickness (mm)	Moisture content (%)	Solubility (%)	Swelling index
G	0.041 ± 0.006^{b}	20.56 ± 4.43^{bc}	73.88 ± 0.194^{c}	12.89 ± 0.072^{b}
I	0.038 ± 0.001^{b}	29.87 ± 2.33^{a}	83.22 ± 1.96^{b}	15.68 ± 2.83^{b}
K	0.067 ± 0.003^{a}	28.43 ± 4.90^{ab}	76.04 ± 2.22^{c}	11.81 ± 0.11^{b}
M	0.057 ± 0.009^{ab}	24.12 ± 0.87^{ab}	79.69 ± 1.8^{bc}	23.96 ± 0.85^{a}
O	0.05 ± 0.001^{b}	31.46 ± 2.79^{a}	98.08 ± 1.92^{a}	25.76 ± 2.21^{a}
Q	0.072 ± 0.004^{a}	15.28 ± 0.39^{c}	76.72 ± 1.28^{c}	12.42 ± 0.31^{b}

edible film, the water content should range from 16.48 to 23.96%.[46] In the present study, it was observed that the films prepared with a hydrophilic polymer, SA, contain more moisture than those prepared from a less hydrophilic polymer, GeG (Table 3). Among films G, I, K, M, O, and Q, films G and Q had the lowest moisture content of 20.5% and 15.2%, respectively. The water retention capacity of film O, 31.4%, was significantly higher ($p \leq 0.05$) than that of all the other films. This is because the hydroxyl and carboxyl groups of sodium alginate form hydrogen bonds with water, increasing the free volume within the polymer matrix. This makes sodium alginate more hydrophilic than gellan gum.[47] However, films fabricated using XG and GeG were sturdier and stronger. Interestingly, despite the presence of two highly hydrophilic polymers, namely guar gum and sodium alginate, film Q has the lowest moisture content, which could be due to a compact crosslinked structure formed by the three gums, restricting water penetration and limiting free volume expansion, hence reducing the water-retaining property of the film.

The moisture content of the OPE-blended films increased with the increase in OPE concentration in both films G and O (Fig. S5A). This can be attributed to the fact that increasing the OPE concentration increases the polyphenolic concentration, which aids the intermolecular interaction between the polymers and the polyphenols.[48] The hydrophilic phenolic compounds present in the extract powder result in an increase in the moisture content of the films.

The solubility of the films followed the same trend as that of moisture content (Fig. S5B). After 24 h, film O showed the highest solubility of about 98.08% in water, whereas film G was only 73.8% soluble in water. Overall, the solubility was also governed by the hydrophilic polymers like guar gum and sodium alginate. For OPE-blended films, the solubility decreased as the OPE concentration increased in films prepared by gellan gum (G, I, and K). However, the solubility of SA-based OPE films did not significantly change with any increase in OPE concentration. In previous reports by Santos *et al.* 2021 (ref. 13) and Amran *et al.* 2024,[49] it has been demonstrated that with the increase in OPE concentration, the solubility of SA-based films decreased. In these studies, only sodium alginate was used along with OPE for the film preparation. This is because of the strong intermolecular bonding of the carboxylic acid groups of OPE with SA. In the present study, the films were prepared using sodium alginate, xanthan gum, and guar gum. No significant change in the solubility shows that the presence of XG and GuG results in the availability of hydroxyl groups, which can interact with water molecules, hence maintaining their solubility.

The swelling index (SI) is another property of the films that was studied. It was seen that the SI of SA-based films was significantly higher than those prepared by gellan gum ($p \leq 0.05$). The SI of film

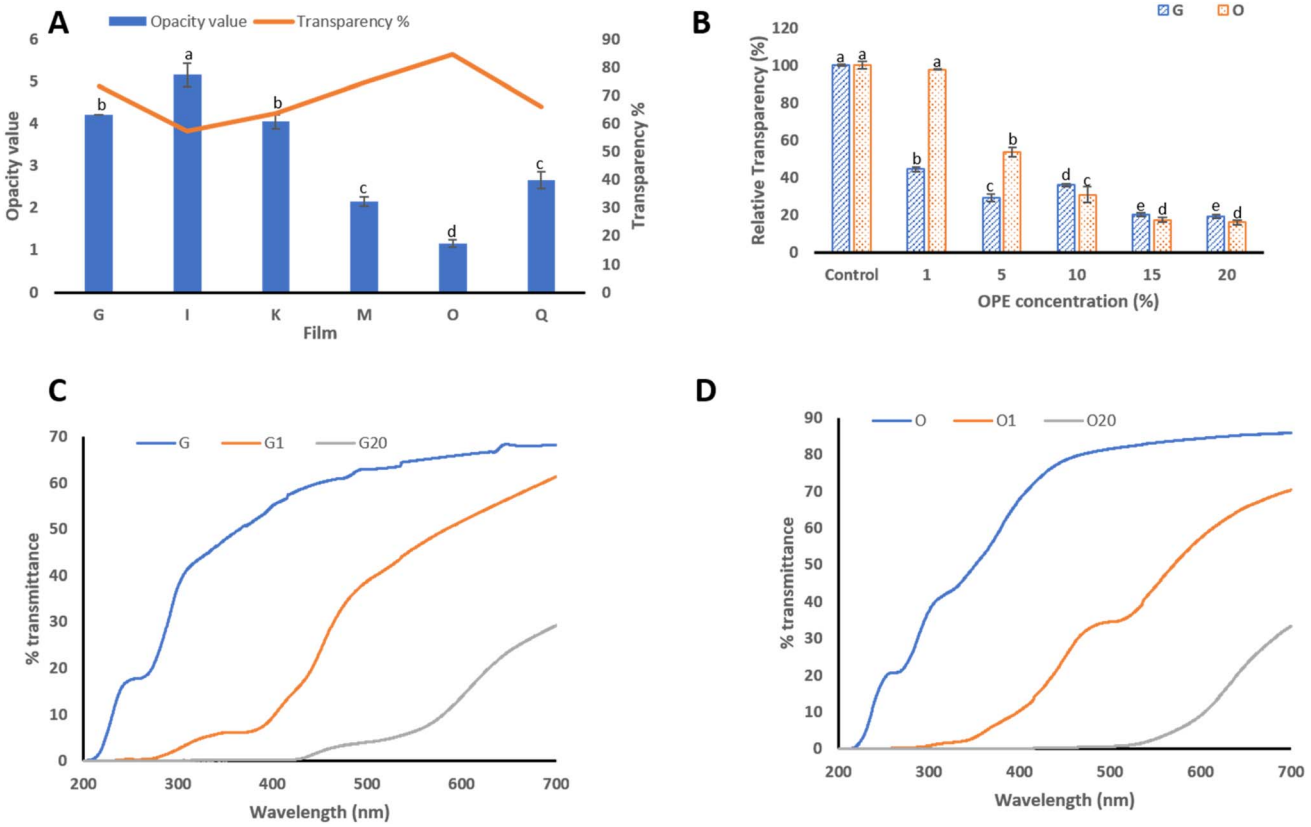

Fig. 2 (A) Optical properties of the films. (B) Relative transparency of films G and O with the increase in OPE concentration. Percentage of transmittance of (C) film G and (D) film O. G, film G without any OPE; G1, film G with 1% OPE; G20, film G with 20% OPE; O, film O without any OPE; O1, film O with 1% OPE; and O20, film O with 20% OPE. Means that share the same letter in the bars of the same pattern are not significantly different at $p \leq 0.05$.

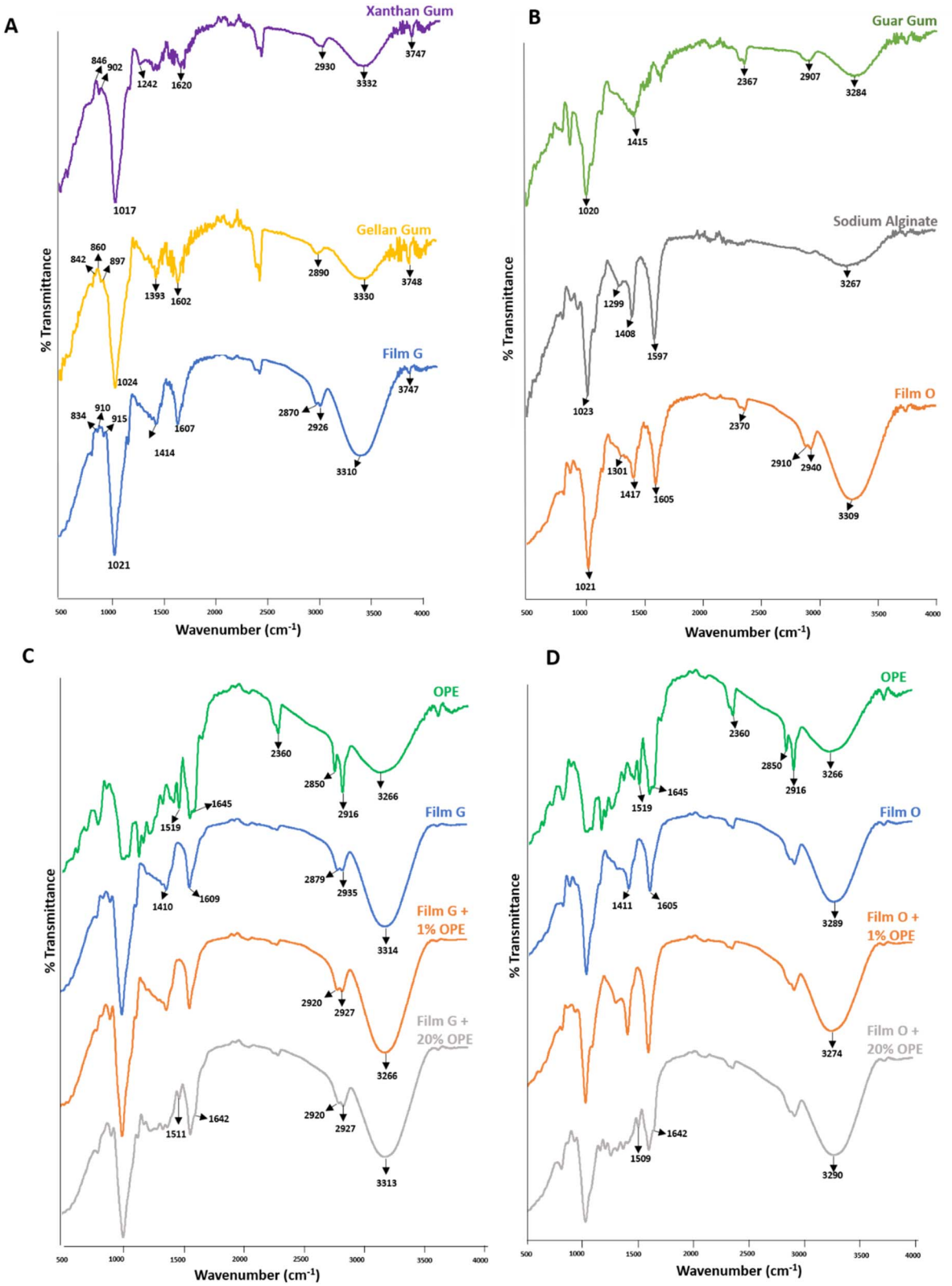

Fig. 3 FTIR spectra of (A) film G and (B) film O with the standards. (C) Spectra of the 1% and 20% OPE-blended film G, alongside blank film G. (D) Spectra of the 1% and 20% OPE-blended film O, along with the blank film O.

O was maximum, 25.76, which could be due to the presence of guar gum and sodium alginate, both of which are hydrophilic and can absorb and retain water, thus resulting in substantial volume expansion (Table 3). Film I shows an intermediate swelling index of 15.6, even after having a hydrophilic polymer, guar gum. This is because of the presence of gellan gum, which forms a more

structured and ordered gel network and limits chain relaxation and the extent of swelling as compared to the alginate-based films.

3.1.3. Optical properties of films. The optical properties of films were determined to check for their transparency, opacity, and UV resistance. Fig. 2A clearly depicts that the transparency of the films (G–Q) increased as their opacity value decreased. Although all the films depicted a transparency (%*T*) of more than 60, film O exhibited the maximum transparency of 84.6%. Films G, I, K, M, and Q have a %T value less than 80%, hence they can be considered translucent, whereas film O, with a %T value more than 80%, can be considered transparent.[50] In general, SA-based films were more transparent than those prepared with GeG. This might be because of the better intermolecular hydrogen bonding between glycerol and SA, which results in more transparent, even, glossier, and flexible films.[51] Gellan gum, however, is a semi-crystalline polymer[1] and forms a compact, crystallizing microstructure within the film, which can scatter light effectively than sodium alginate.

The transparency of the OPE-blended films decreased significantly ($p \leq 0.05$) with the increase in OPE concentration from 1% to 20% (Fig. 2B). This was further validated by Fig. S4, showing the darkening of the color in films G and O, as the OPE concentration was increased from 1% to 20%, and the results are consistent with previous reports.[13] This could be attributed to the light-scattering effect, according to which the optical properties of the films depend on the concentration of the extract used.[52] Onion peel extract contains many polyphenols, which act as chromophores and absorb UV-vis spectra. This results in the retardation of light propagation, hence reducing its transparency.[53] Furthermore, the optical clarity depends on the thickness of the film, as thicker films present a longer optical path length for light to traverse, hence transmitting less light.[54]

In general, to reduce the spoiling of light-sensitive food materials, packaging materials with low transmittance (%) are preferred.[55] This would enhance the shelf life of food products. The addition of OPE in the films decreased the % transmittance of the films. The transmittance (%) of the films incorporated with OPE decreased in the UV range (200–400 nm) with the increase in the OPE concentration of 1–20%. Film G1, containing 1% OPE, showed significant absorption across the UVC region (200–280 nm). When the OPE concentration in film G was increased to 20%, the UV radiations in the entire range (200–400 nm) were absorbed (Fig. 2C). Similarly, film O1 absorbed UVC and a part of UVB (200–340 nm), and O absorbed 20% of radiations in the entire UV spectrum (Fig. 2D). Thus, we can infer that 20% OPE-blended films exhibit UV absorption activity, hence proving to be excellent UV barrier materials. Similar results have been reported by Li *et al.* 2022.[55]

3.2. TPC of OPE and OPE-blended films

Onion peel extract contains polyphenols, which are responsible for its antioxidant activity.[56] Thus, the total phenolic content of both the free OPE and OPE-blended films was determined (Table S3). The TPC of OPE was calculated to be 393 mg GAE per g. In the case of OPE-blended films, the TPC increased with the increase in OPE concentration. This result was consistent with that reported by Moradi *et al.* 2023.[15] The films with high solubility showed a higher TPC value, owing to their ability to evenly disperse OPE in water. Antioxidant films can act as a barrier and prevent the food products from oxidation and deterioration, hence maintaining their freshness.[57]

3.3. Antioxidant potential of OPE

The antioxidant activity was determined using the DPPH method. The scavenging activity was determined by measuring the reduction of DPPH free radicals by hydrogen atom donation or electron transfer from an antioxidant compound.[29] The radical scavenging activity was calculated to be 66%. A previous work on onion peels reports their DPPH scavenging activity to be 62.66%.[58]

Moreover, the IC_{50} value of OPE was determined to be 17 μg mL^{-1}. Similar results were obtained by Khalili *et al.* 2022,[29] where the IC_{50} value of red onion peel ethanolic extract was determined to be 22.4 μg mL^{-1}. The results indicate that the OPE could be used as a potent antioxidant in the food industry.

3.4. FTIR characterization of films

The strong absorption bands near 3330 cm^{-1} indicate the stretching caused by intermolecular hydrogen bonds.[1] Fig. 3A shows the comparative FTIR spectra of film G with its individual constituents, XG and GeG. Film G shows a shift in the –OH vibrations from 3330 cm^{-1} and 3332 cm^{-1} to 3310 cm^{-1}. Moreover, this peak of film G is broader and stronger than those of XG and GeG (Fig. 3A). This is attributed to the increase in intermolecular hydrogen bonding between GeG and XG during film preparation.[41] These could also be due to glycerol present in the films. The peaks around 2930 cm^{-1} (in XG) and 2890 cm^{-1} (in GeG) correspond to the aliphatic –CH stretching and are seen to be merged in the FTIR chromatogram of film G. The carbonyl band at 1620 cm^{-1} also shifted to 1607 cm^{-1} for film G, further indicating the increase in H bonds due to intermolecular bonding between glycerol and polymers (XG and GeG). The band around 1024 cm^{-1} indicates the presence of C–O stretching from the polysaccharide rings. This is consistent with all the samples. The bands in the fingerprint region between 800 and 1000 cm^{-1} fall within the range where glycosidic linkage occurs. In this region, the change in the peak pattern of film G indicates the combination of structural elements of XG and GeG during film formation. The spectral changes of film G, in the region 1000–2200 cm^{-1}, further prove the synergistic interaction between the two polymers, along with glycerol.

Similarly, in Fig. 3B (comparing the FTIR spectra of film O with GuG and SA), the peaks around 3000–3500 cm^{-1} indicate the presence of –OH groups on the surface. The broad peak in the spectra of film O could be attributed to the increase in intermolecular hydrogen bonding between guar gum and sodium alginate, accompanied by glycerol.[59] The peak around 2900 cm^{-1} corresponds to the –CH stretching by the polysaccharide backbones of the polymers and glycerol.[60] Interestingly, a new peak around 2940 cm^{-1} appeared in the

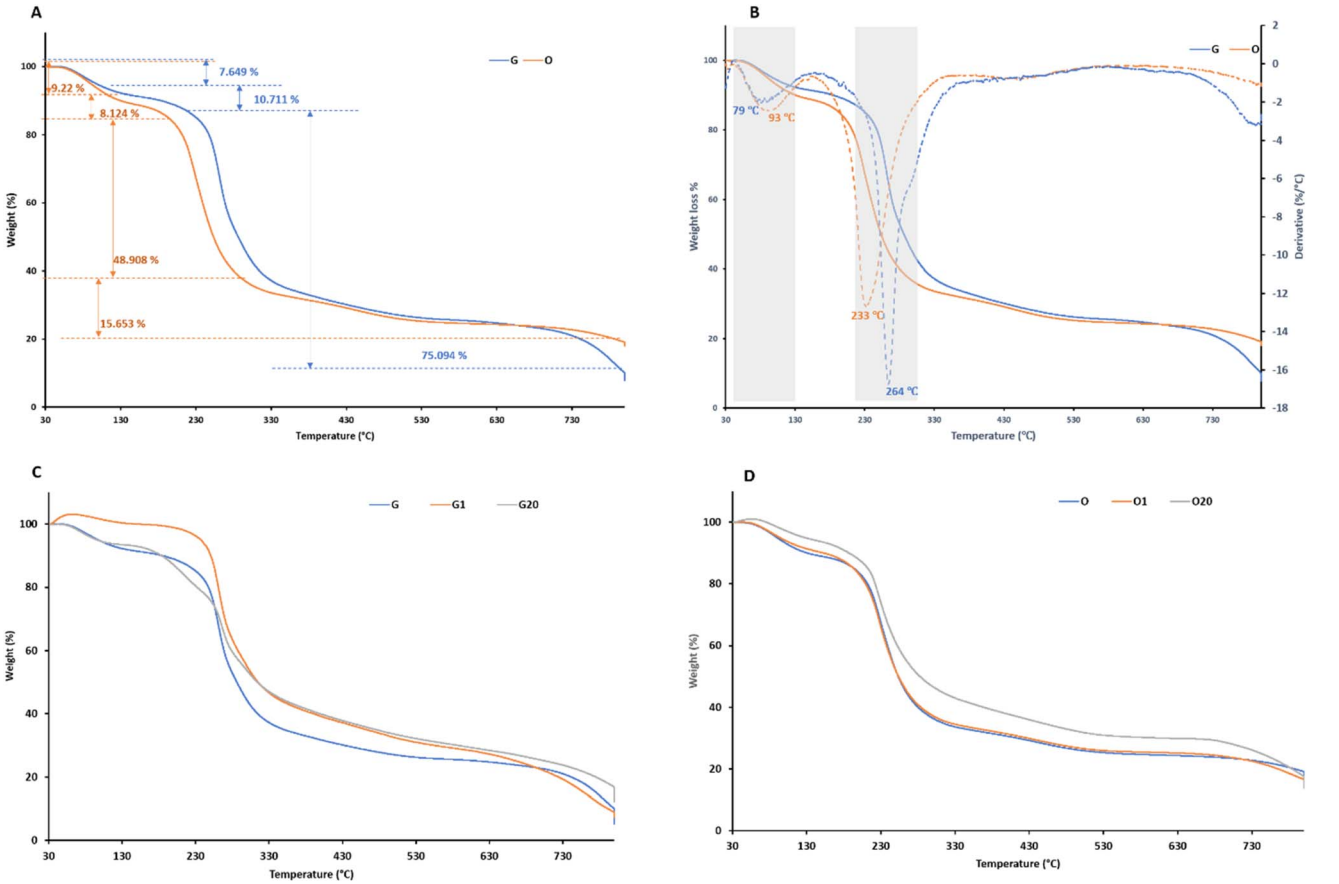

Fig. 4 (A) TGA thermograms of films G and O. (B) Graph showing DTG data for films G and O. TGA thermogram of the (C) 1% and 20% OPE-blended film G with blank film G and (D) 1% and 20% OPE-blended film O with blank film O. G, film G without any OPE; G1, film G with 1% OPE; G20, film G with 20% OPE; O, film O without any OPE; O1, film O with 1% OPE; and O20, film O with 20% OPE.

chromatogram of film O, which could be a result of intermolecular intercalation of the two polymers. The peak around 1597 cm^{-1} indicates the presence of an asymmetric carboxylate anion (COO–) in sodium alginate. A similar peak is present in the spectrum of film O at 1600 cm^{-1}, indicating the incorporation of SA into the films. The peaks around 1300 cm^{-1} and 1400 cm^{-1} for both SA and film O are associated with the C–O stretching of carboxyl groups and the symmetric stretching of COO– anion.[60] The peak near 1020 cm^{-1} indicates the C–O stretching from the polymers used. The fingerprint region also denotes several changes in peaks, further proving the combination of GuG, SA, and glycerol to produce film O.

In case of the onion peel extract-blended films, the FTIR spectra of 1% OPE- and 20% OPE-containing films were compared with those of the blank films (having no OPE) and OPE (Fig. 3C and D). The band in the OPE spectra at 3266 cm^{-1} corresponds to the free OH groups of flavonoids and phenols present in the extract.[61] This peak broadens and intensifies for OPE-blended films because of the combined effect of hydrogen bonds between the polymers, glycerol, and OPE. The peaks around 2850 cm^{-1} and 2916 cm^{-1} for OPE correspond to the aliphatic and aromatic CH bonds, respectively. A peak around 1645 cm^{-1}, which is absent in the spectrum of film G but can be faintly seen in the spectrum of OPE-blended films, could correspond to the bending vibrations of amines in the OPE. A characteristic peak of OPE was also identified at 1519 cm^{-1}, which was present in OPE-blended films. The presence of various biomolecules like polyphenols, lipids, and proteins was confirmed by the presence of peaks in the region between 500 and 1600 cm^{-1}.[62] These peaks can also be seen in OPE-blended films, reflecting the interaction of OPE embedded within the film structure. The concentration of the OPE affects the peak intensities and broadness of the samples. The characteristic peaks of the polymers, as discussed above, are present in all the films. The incorporation of OPE into film O can be similarly explained.

3.5. Thermal stability of films

To analyze the temperature stability of the prepared films, TGA was performed. The percentage of weight loss was determined with respect to temperature (Fig. 4A). The TGA of films G and O was compared. The initial degradation step resulted in a 7.6% and 9.2% decrease in the weight of films G and O, respectively (Fig. 4A). This initial weight loss corresponds to the loss of moisture/volatile compounds from the films. For film O, the decomposition rate was faster and in a narrower temperature range than that of G. Major degradation occurred between 200 and 300 °C, where ~50% and 49% weight loss occurred in films

G and O, respectively. A second decomposition step was observed between 300 and 600 °C, showing slow but continuous degradation. Above 600 °C, some residual amounts of the films were still present, indicating the presence of thermally stable components or the formation of char.

In Fig. 4B, the dashed line denotes the DTG curves of both film samples, which clearly denote the two-step degradation of films G and O. In the first degradation step, a weight loss occurred at temperatures lower than 150 °C, which denotes the removal of structurally bound water molecules and the degradation of glycerol molecules.[14] In the second degradation step, the respective polymers degraded rapidly at 264 °C and 233 °C for films G and O, respectively.[63]

The TGA curve for film G blended with 1% and 20% OPE was compared with that of blank film G (Fig. 4C). The first degradation step was again observed below 150 °C, which represented the initial weight loss and glycerol degradation. However, the initial degradation of G1 was slower than that of G20 and control film G. The second major degradation stage was similar to all three films, where the polysaccharide backbone of the films degraded. However, the rate of decomposition was slower for OPE-blended films than for the control film. This might be due to the strong intermolecular force between the polymers and the OPE, which resulted in a strong, compact, and thermally stable biomaterial, which required more energy for its breakdown. Similar results were reported by Santos *et al.* 2021,[13] where the addition of polyphenol-rich extracts enhanced the thermal stability of alginate-based films.

In the case of film O, the thermal stability of the film incorporated with OPE was more than that of the control film (Fig. 4D). However, no visible difference was observed in the thermostability of control films O and O1. The abrupt weight loss of 1% OPE-blended G and O films is probably due to the degradation of the limited phenolic compounds present, compared to the greater phenolic content in 20% OPE-blended films.[14]

3.6. XRD analysis of films

To analyze the crystallinity or amorphous nature of the films, XRD analysis was performed on films G and O. The crystalline nature of the OPE-blended films was also studied. Fig. 5 shows an overlay of diffractograms of GeG, XG, and film G (Fig. 5A); and GuG, SA, and film O (Fig. 5B). In Fig. 5A, xanthan gum shows the presence of certain peaks at 19°, 32°, and 45°. Although the peak at 19° confirms the amorphous nature of XG, the peaks at 32° and 45° may be due to the presence of some inorganic salts like NaCl in the XG, as food-grade XG was used in the experiments. Gellan gum showed a semi-crystalline nature as discussed by Agarwal *et al.* 2023.[1] Film G showed the disappearance of many peaks of XG and GeG. A peak at 19° was present for film G, indicating its amorphous nature. Interestingly, a new peak emerged at 28°. This disappearance of peaks and emergence of new peaks might correspond to the formation of new bonds and intermolecular interactions between GeG and XG during the thermal gelation process.[41] The peak at 44° might correspond to the crystalline nature of the films, attributed to the addition of glycerol in the films during their preparation.[1]

In Fig. 5B, the semi-crystalline nature of guar gum was confirmed by a broad peak at 19°. The peaks at 9° and 15° might correspond to its crystalline polysaccharide portion. For SA, two crystalline peaks at 13° and 21° were observed in the XRD diffractogram. Film O, which was a blend of GuG and SA, showed a characteristic peak at 21°, which was similar to that of SA. Another peak at 44° was observed for film O, which might correspond to the crystalline nature of glycerol, which was added as a plasticizer in the film preparation. However, all other peaks disappeared in the film diffractogram. This change and disappearance of the peaks confirm the synergistic interaction and strong binding between GuG and SA. These results were consistent with the study results of Cheng *et al.*, 2021,[64] where gum ghatti was blended with sodium alginate to form films.

In Fig. 5C and D, the diffractogram of OPE shows peaks at 21° and 24°, indicating the presence of crystalline cellulose, which is primarily present in the plant cell walls.[65] For OPE-blended films, a merged peak can be seen at 22°, which might be due to the incorporation of OPE into films G and O. This confirms the interaction of polymers with OPE in the films. The addition of OPE resulted in peak broadening and reduced intensity of characteristic diffraction peaks, indicating the disruption of ordered crystalline domains and an increase in amorphous regions.

3.7. Mechanical characterization of films

The flexibility and strength of the films were determined by calculating their tensile strength, Young's modulus, and elongation at break. A universal testing machine (UTM) was utilized for this purpose. The tensile strength of the films prepared with only xanthan gum (film A) and guar gum (film C) was determined to be 0.68 N mm^{-2} and 3.6 N mm^{-2}, respectively (Table 4). The tensile strength and elongation at break increased significantly when these polymers were blended with gellan gum and sodium alginate, respectively ($p \leq 0.05$). Out of the blended polymer matrices, the tensile strength (TS) of film G was maximum, *i.e.*, 26.84 N mm^{-2}, whereas the TS was only 4 N mm^{-2} for film Q. The findings are similar to those reported by Rukmanikrishnan *et al.*, 2020.[66] This represents that the tensile strength of film G was maximum, whereas film Q was the weakest. In general, the films made with gellan gum were stronger and had a higher tensile strength than that of the films made using sodium alginate. This can be attributed to the formation of a rigid gel network by gellan gum, which restricts the mobility of polymer chains and reduces free volume. However, the films made with SA were more ductile and had a higher EAB value than that of gellan gum films. This can be proved by the fact that film O had the maximum elongation at break (EAB) value of 36.35%, whereas films G, I, and Q were the least elongated after stretching. The difference between the mechanical properties of GeG and SA-based films has also been previously reported by Carrêlo *et al.*, 2022 (ref. 67) and Ajam *et al.* 2024.[47] Young's modulus of the films decreased with the decrease in their tensile strength. This could be attributed to enhanced polymer chain mobility, resulting in a softer material. The EAB of the films could also be related to the moisture content of the films. The film with high moisture (O) has the highest EAB value. This could be because water molecules act as an additional

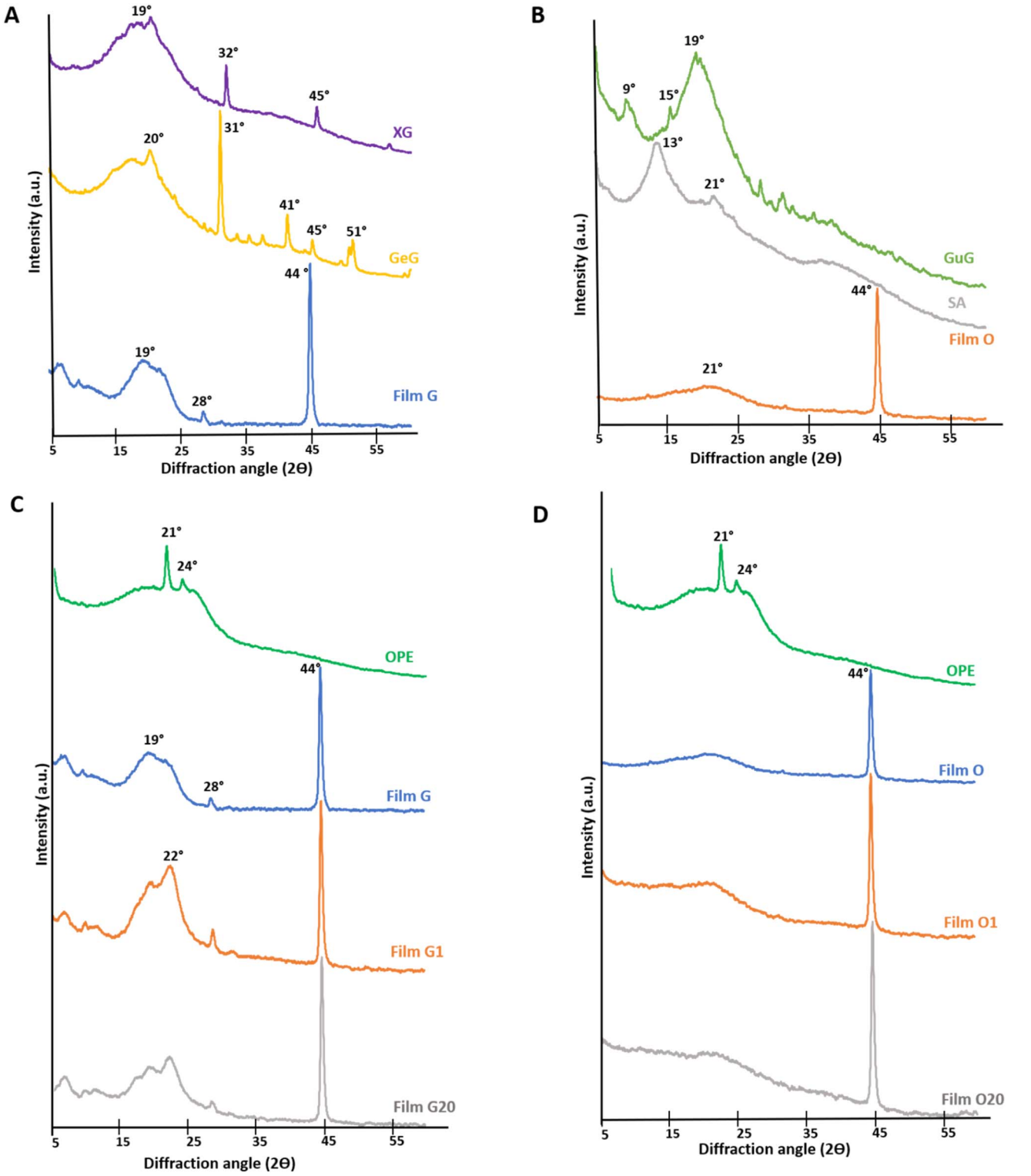

Fig. 5 X-ray diffractogram of (A) film G and (B) film O with the standards. Diffractogram of (C) 1% and 20% OPE-blended film G, alongside blank film G and (D) 1% and 20% OPE-blended film O, along with the blank film O.

plasticizer (other than glycerol) and increase the ductility and flexibility of the films.[68] Moreover, with the increase in moisture, the hydrogen bonds between the polymers can be easily disrupted, leading to the formation of a weak, but softer film.[69,70] Thus, the mechanical properties of the films were determined by network rigidity and moisture-induced plasticization.

In OPE-blended films, a similar trend of mechanical properties was seen with respect to the moisture content of the films

Table 4 Mechanical properties of the films. Means sharing different letters within a column indicate a significant difference ($p < 0.05$)

Film	TS (N mm^{-2})	YM (MPa)	EAB (%)
A	0.684 ± 0.005^{a}	0.221 ± 0.21^{a}	5.16 ± 1.2^{a}
C	3.605 ± 0.86^{a}	0.241 ± 0.011^{a}	14.6 ± 1.6^{cd}
G	26.84 ± 7.6^{d}	3.3 ± 0.215^{c}	8.65 ± 1.4^{abc}
I	23.96 ± 6.10^{cd}	3.8 ± 0.937^{c}	6.75 ± 0.459^{ab}
K	21.71 ± 1.11^{cd}	1.3 ± 0.522^{b}	13.7 ± 3.5^{bcd}
M	10.04 ± 2.77^{ab}	0.59 ± 0.04^{ab}	18.34 ± 2.34^{d}
O	15.45 ± 6.08^{bc}	0.47 ± 0.016^{ab}	36.35 ± 6.3^{e}
Q	4.00 ± 0.48^{a}	0.525 ± 0.012^{ab}	7.5 ± 0.1^{abc}

(Fig. S6A and B). Water, which acts as a secondary plasticizer in the films, increases the free volume within the polymer, increasing polymer chain mobility and making the film more flexible.[45] Since the moisture content of the films increased when 20% OPE was incorporated into the films, the EAB increased from 8.7% (blank G film) to 15.7% (G20 film) for film G (Fig. S6A) and from 36.1% (blank O film) to 45.9% (O20 film) for film O (Fig. S6B). This also resulted in simultaneous decreases of 28% and 21% in the tensile strength of films G and O, respectively. This depicts that OPE-blended films attained a higher flexibility, while they were less strong than the blank films. The decrease in tensile strength with the increase in OPE concentration was also observed by Santos *et al.* 2021 (ref. 13) and Gulati *et al.* 2023 (ref. 14) when onion peel extract of different concentrations was added to sodium alginate and methylcellulose films. Reduced tensile strength is indicative of an increased free volume and porosity within the material's matrix. The incorporation of extracts into the polymer disrupts its structural integrity, expanding free volume and introducing disorders, thereby diminishing intermolecular interactions within the polymer.[14] This increased free volume results in weaker intermolecular bonds, and the polymer chain attains more flexibility, increasing EAB. However, beyond a certain concentration of OPE, the EAB started decreasing, although the decrease was insignificant. A similar trend in the increase of EAB with the increase in OPE concentration was also observed by Amran *et al.*, 2024.[49]

3.8. Relationship between the structural, thermal, and mechanical properties of OPE-blended films

The FTIR spectra and XRD patterns demonstrate the molecular interactions and the structural organization of molecules present in OPE, with the polymer matrix, which, in turn, governs the thermal and mechanical behaviors of the films. The FTIR spectra of OPE-blended films show slight shifts of the –OH stretching band (~3200–3400 cm^{-1}) and changes in the fingerprint regions, which confirm the formation of phenolic–polymer hydrogen bonds between OPE polyphenols and polysaccharide functional groups. These hydrogen bonds restrict the molecular chains' movement, which, in turn, hinders crystallite growth.[71] In OPE-blended films, the crystallinity of the films decreases along with the increase in OPE concentration, which increases the free volume, hence resulting in decreased tensile strength and increased flexibility. TGA data support this structural interpretation, where reduced crystallinity resulted in earlier onset of thermal degradation (in G20) and broader degradation steps (O20). This could be attributed to increased molecular mobility and weaker intermolecular cohesion with OPE incorporation.

3.9. Antimicrobial activity of OPE-blended films

Films G, I, K, M, O, and Q with different concentrations of OPE (0, 1, 5, 10, 15 and 20%) were tested against most common pathogens, namely *E. coli* (gram −ve) and *S. aureus* (gram +ve), an opportunistic pathogen, *B. megaterium* (gram +ve) and a fungus, *C. albicans* (Fig. S7E). The antimicrobial activity was analyzed by observing the zone of inhibition formed around the film sample. All the films exhibited a certain level of antimicrobial activity against all three pathogens. This can be attributed to the fact that onion peels contain several bioactive compounds such as quercetin, kaempferol, and luteolin, which are antimicrobial in nature.[72] The antimicrobial effect can be exerted through various mechanisms, namely, disruption of microbial cell membranes, increased membrane permeability, generation of reactive oxygen species, metabolic enzyme inactivation, and DNA oxidation, leading to cell death.[73,74] Increased moisture in OPE-containing films facilitates phenolic mobility, thereby improving their interaction with microbial cells. Interestingly, all the films showed a greater inhibition zone against *S. aureus* and the smallest zone towards *E. coli*. film G, at 20% OPE concentration, showed maximum antimicrobial resistance towards all four pathogens. The results were comparable to film I in the case of bacterial samples. The zone of inhibition was not calculated and compared because sodium alginate-based films (M, O, and Q) gathered moisture from the agar plate and were swollen sideways, leading to an illusion of increased zone of inhibition (Fig. 6). Additionally, the antimicrobial activity of OPE was higher against Gram-positive bacteria than Gram-negative bacteria. This is because of the changes in the cell wall of the bacteria. Gram-negative bacteria contain a lipopolysaccharide layer in their outer membrane, which aids in antibiotic resistance against various antimicrobial agents.[75] Similar results were observed and reported by Mardani *et al.* 2023.[76] Interestingly, the films also showed antifungal properties by inhibiting the growth of *C. albicans* (Fig. 6). Gellan gum-based films showed a significant zone of inhibition against the eukaryotic fungi as compared to sodium alginate-based films.

The MIC and MBC of OPE were also determined against *E. coli*, *B. megatrium*, *S. aureus* and *C. albicans*, and were compared to that of SB. The MIC of sodium benzoate was determined by the agar dilution method to be 15 mg mL^{-1}, 18 mg mL^{-1}, 35 mg mL^{-1}, and 10 mg mL^{-1} for *E. coli*, *B. megatrium*, *S. aureus*, and *C. albicans*, respectively. However, with the broth dilution method, the MIC values slightly shifted to 30 mg mL^{-1} for *S. aureus* and 12 mg mL^{-1} for *C. albicans*.

The MIC value of OPE determined by the agar dilution method was 8 mg mL^{-1}, 8 mg mL^{-1}, 1 mg mL^{-1}, and 3 mg mL^{-1} for *E. coli*, *B. megatrium*, *S. aureus*, and *C. albicans*, respectively.

Further, the MBC values for all the microbes were determined using the broth dilution method for both SB and OPE.

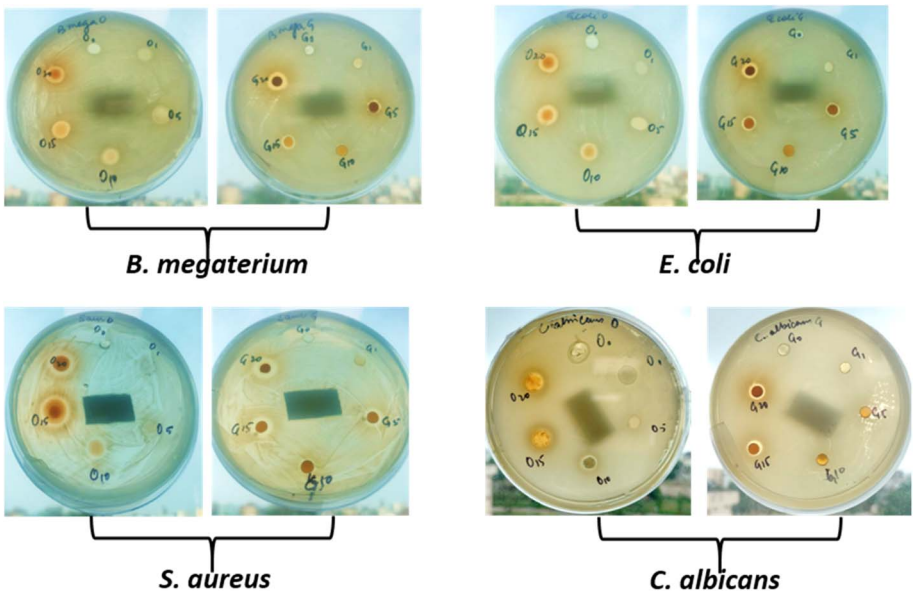

Fig. 6 Antimicrobial activity of different OPE-blended films on pathogenic bacteria and fungi. The films with different concentrations of OPE were placed as discs on the Petri plate. G, film G without any OPE; G1, film G with 1% OPE; G5, film G with 5% OPE; G10, film G with 10% OPE; G15, film G with 15% OPE; and G20, film G with 20% OPE. Similar concentrations were used and marked for film O.

The MBC value was determined to be 25 mg mL^{-1}, 25 mg mL^{-1}, 40 mg mL^{-1} and 35 mg mL^{-1} for sodium benzoate and 10 mg mL^{-1}, 10 mg mL^{-1}, 3 mg mL^{-1} and 3 mg mL^{-1} for OPE, against *E. coli*, *B. megatrium*, *S. aureus*, and *C. albicans*, respectively. The results confirm that the OPE is a more effective antimicrobial agent, and thus, can be effectively used to replace the chemical preservative, sodium benzoate, in the food industries.

3.10. Preservative effect of onion peels

In the literature, onion peels, as a sole compound or in combination with other compounds, have been proven to increase the nutritional quality, shelf life, mineral content, and antioxidant potential of various food products.[77] Reports have also indicated the use of onion peels as a colorant in jellies and candies, owing to their bright red color.[78] However, only a few studies have shown the use of onion peels or their extracts as a natural preservative for food products. Mostly, OPE has been used for the preservation and shelf-life enhancement of beef,[79–82] pork,[83] chicken,[15,84] and fish products.[85] A few reports also demonstrate the use of OPE for the enhancement of the shelf life of multigrain bread[86] and soybean oil.[87] However, the use of OPE as a preservative for perishable fruits has not yet been reported.

Sodium benzoate is the most common food preservative used in the food industry. It is a bacteriostatic and fungistatic compound, which helps in preventing the spoilage of beverages, liquid medications, and some personal care products. However, reports have indicated that it can lead to fertility issues and hormone disruption, and can even cause oxidative stress.[88] Therefore, OPE can serve as a natural and sustainable preservative for food items. To study its antimicrobial activity in comparison to sodium benzoate, *E. coli*, *B. megatrium*, *S. aureus*, and *C. albicans* were treated with equal concentrations of both OPE and sodium benzoate (Fig. S7A–D). Interestingly, OPE showed a larger zone of inhibition as compared to sodium benzoate for the tested bacterial cultures. Sodium benzoate was observed to be inactive against *S. aureus* but more active than OPE against the fungus, *C. albicans*. To examine the preservative capability of onion peel extract, grapes were dipped in the film casting solution containing 1% and 20% OPE extract. The coated grapes were then kept at two different temperatures (4 °C and 25 °C) to evaluate their shelf lives. After 15 days of storage at 25 °C, the grapes coated with the blank casting solution of films G and O (no OPE), exhibited noticeable weight loss and shrinkage. In contrast, the grapes having OPE-blended coatings were less shrunk than the control grapes and more palatable. Interestingly, the grapes kept at 4 °C were palatable even after 15 days of incubation (Fig. 7A). The grapes coated with the 20% OPE-blended film G solution and incubated at 4 °C were fresh, flaccid, and hydrated even after 15 days; however, the grapes coated with the film O solution at the same temperature and OPE concentration were somewhat shrunk after 15 days. This further proves that film G has better water repellent and less moisture absorption qualities, and can be used with onion peel extract to increase the shelf life of perishable fruits and vegetables. To remove the coatings, fruits can be simply washed under water, or can be eaten as a whole, with the coating.

The films were also used to store blueberries. The physical appearance and weight of the blueberries were checked after 15 days of incubation at room temperature and 4 °C (Fig. 7B and S8). It was observed that although the blueberries stored at 4 °C did not show any change in their physical appearance even after 15 days of incubation, those at 25 °C shrank due to loss of moisture. In the control group of fruits, a weight loss of 71.1% and 43.6% was observed at 25 °C and 4 °C, respectively (Fig. 7B). At both temperatures, it was observed that with the increase in OPE concentration in the films (G and O), the percentage of weight

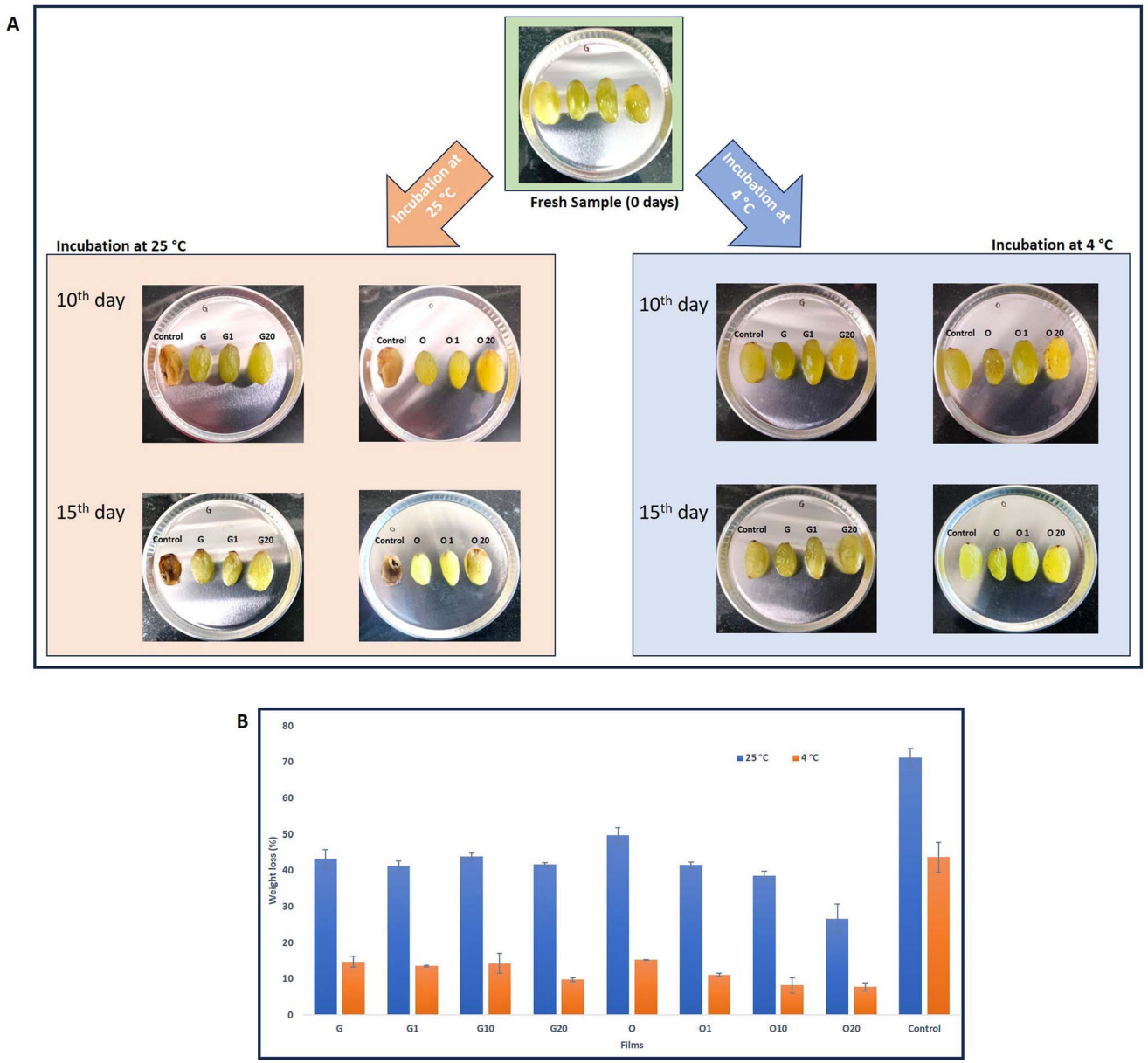

Fig. 7 (A) Preservative effect of the OPE-blended film-forming solution on grapes. (B) Weight loss (%) of blueberries after 15 days of incubation in film packages at 4 °C and 25 °C. Control, without any coating or packaging; G, film G without any OPE; G1, film G with 1% OPE; G10, film G with 10% OPE; G20, film G with 20% OPE; O, film O without any OPE; O1, film O with 1% OPE; O10, film O with 10% OPE; and O20, film O with 20% OPE. The mean values that share the same letter in the bars of the same pattern are not significantly different at $p \leq 0.05$.

loss of the berries decreased, when compared to the control group (blueberries not packed) and those packaged in the blank films (without any OPE incorporated). Thus, the results indicate that the films can also be used as packaging materials, reducing the moisture loss from perishable fruits and other food items.

4. Conclusions

This study demonstrated the valorization of onion peels into edible, sustainable films, depicting excellent mechanical and preservative properties. The film prepared by blending 0.3% XG with 0.3% GeG exhibited the highest tensile strength of 26.84 N, whereas the film prepared by blending 0.5% SA and 0.3% GuG showed maximum ductility with an EAB value of 36.3%. The incorporation of OPE (1–20% w w^{-1}) decreased the tensile strength but increased the EAB of the films while imparting antioxidant and antimicrobial activities to the films against *E. coli*, *B. megaterium*, *S. aureus*, and *C. albicans*. The OPE-containing film casting solution effectively increased the shelf life of grapes up to 15 days at room temperature, while packaging blueberries in OPE-containing films improved moisture retention, confirming their potential as potent bioactive preservatives. OPE-based films can thus provide an eco-friendly solution for food preservation and waste valorization within the framework of circular bioeconomy.

Conflicts of interest

The authors declare that there is no conflict of interest.

Data availability

The data supporting this article have been included as part of the supplementary information (SI). Supplementary information is available. See DOI: https://doi.org/10.1039/d5fb00790a.

Acknowledgements

The authors acknowledge BRIC-National Agri-Food and Biomanufacturing Institute (Formerly Center of Innovative and Applied Bioprocessing), Mohali, Punjab, under Department of Biotechnology (DBT), Govt. of India for constant support and motivation throughout this study. The authors also thank the researchers and staff members of BRIC-NABI, Mohali for their assistance and cooperation over the course of the study.

References

1 N. Agarwal, Jyoti, M. Thakur, B. B. Mishra and S. P. Singh, *Environ. Technol. Innovation*, 2023, **31**, 103231.
2 V. Kola and I. S. Carvalho, *Food Biosci.*, 2023, **54**, 102860.
3 M. Kumar, M. D. Barbhai, M. Hasan, S. Dhumal, S. Singh, R. Pandiselvam, N. Rais, S. Natta, M. Senapathy, N. Sinha and R. Amarowicz, *J. Food Sci.*, 2022, **87**, 4289–4311.
4 F. Stoica, R. N. Ratu, I. D. Veleşcu, N. Stănciuc and G. Râpeanu, *Trends Food Sci. Technol.*, 2023, **141**, 104173.
5 J. Y. Ng, S. Obuobi, M. L. Chua, C. Zhang, S. Hong, Y. Kumar, R. Gokhale and P. L. R. Ee, *Carbohydr. Polym.*, 2020, **241**, 116345.
6 S. Naji-Tabasi, M. Shahidi-Noghabi and A. M. Dovom, *J. Sol-Gel Sci. Technol.*, 2023, **105**, 637–649.
7 C. C. Kandar, M. S. Hasnain and A. K. Nayak, in *Advances and Challenges in Pharmaceutical Technology*, Elsevier, 2021, pp. 1–44.
8 E. Theuwissen and R. P. Mensink, *Physiol. Behav.*, 2008, **94**, 285–292.
9 L. Brown, B. Rosner, W. W. Willett and F. M. Sacks, *Am. J. Clin. Nutr.*, 1999, **69**, 30–42.
10 Q. Lin, Y. Si, F. Zhou, W. Hao, P. Zhang, P. Jiang and R. Cha, *Carbohydr. Polym.*, 2024, **323**, 121414.
11 B. Zhang, W. Lan and J. Xie, *Int. J. Biol. Macromol.*, 2022, **223**, 1539–1555.
12 B. Jadach, W. Świetlik and A. Froelich, *J. Pharm. Sci.*, 2022, **111**, 1250–1261.
13 L. G. Santos, G. F. A. Silva, B. M. Gomes and V. G. Martins, *Biocatal. Agric. Biotechnol.*, 2021, **35**, 102096.
14 M. Gulati, K. M. P. S. and J. P. Reddy, *Food Bioprocess Technol.*, 2023, **16**, 2328–2342.
15 D. Moradi, Y. Ramezan, S. Eskandari, H. Mirsaeedghazi and M. Javanmard Dakheli, *Food Packag. Shelf Life*, 2023, **35**, 101012.
16 A. Ju and K. Bin Song, *Int. J. Food Sci. Technol.*, 2020, **55**, 1671–1678.
17 J. Puišo, J. Žvirgždas, A. Paškevičius, S. Arslonova and D. Adlienė, *Antibiotics*, 2024, **13**, 441.
18 T. Liang, G. Sun, L. Cao, J. Li and L. Wang, *Food Hydrocolloids*, 2018, **82**, 124–134.
19 D. Devi, S. Kumar and A. Mukherjee, *Food Humanit.*, 2024, **2**, 100223.
20 İ. Uçak, P. Yerlikaya, R. Khalıly and A. K. m. Abuibaid, *Eurasian J. Food Sci. Technol.*, 2019, **3**, 40–48.
21 S. Pirsa, M. Bener and F. B. Şen, *Food Chem.*, 2024, **445**, 138721.
22 P. Thivya, Y. K. Bhosale, S. Anandakumar, V. Hema and V. R. Sinija, *Food Chem.*, 2022, **390**, 133221.
23 C. Wang, Y. Lu, Z. Li, X. An, Z. Gao and S. Tian, *Polymers*, 2022, **14**, 2986.
24 S. Rajendran, V. Rathinam, M. Kandasamy, S. S. Arumugam, A. Malik and A. A. Khan, *J. Mol. Struct.*, 2024, **1316**, 138986.
25 E. Boccalon, G. Viscusi, E. Lamberti, F. Fancello, S. Zara, P. Sassi, M. Marinozzi, M. Nocchetti and G. Gorrasi, *Appl. Surf. Sci.*, 2022, **593**, 153319.
26 C. L. De Dicastillo, R. Navarro, A. Guarda and M. J. Galotto, *Antioxidants*, 2015, **4**, 533–547.
27 M. Hamid Salim, Y. Abdellaoui, M. Mennani, A. Soumare, L. Díaz-Jimenéz, M. El Achaby and Z. Kassab, *J. Appl. Polym. Sci.*, 2025, **142**, e56705.
28 S. N. Idris and S. A. Othman, *Springer Proc. Phys.*, 2023, **294**, 405–412.
29 S. Khalili, M. R. Saeidi Asl, M. Khavarpour, S. M. Vahdat and M. Mohammadi, *J. Food Meas. Charact.*, 2022, **16**, 3578–3588.
30 J. Ghaderi, S. F. Hosseini, N. Keyvani and M. C. Gómez-Guillén, *Food Hydrocolloids*, 2019, **95**, 122–132.
31 E. Drago, R. Campardelli, A. Lagazzo, G. Firpo and P. Perego, *Polymers*, 2023, **15**, 2231.
32 J. E. Lee, J. T. M. Jayakody, J. Il Kim, J. W. Jeong, K. M. Choi, T. S. Kim, C. Seo, I. Azimi, J. M. Hyun and B. M. Ryu, *Foods*, 2024, **13**, 3151.
33 L. K. Narnoliya, N. Agarwal, S. N. Patel and S. P. Singh, *J. Microbiol.*, 2019, **57**, 900–909.
34 L. Hu, W. Yu, Y. Li, N. Prasad and Z. Tang, *BioMed Res. Int.*, 2014, **2014**, 341291.
35 S. Galus and J. Kadzińska, *Food Hydrocolloids*, 2016, **52**, 78–86.
36 T. Gasti, S. Dixit, R. B. Chougale and S. P. Masti, *Sustainable Food Technol.*, 2023, **1**, 390–403.
37 J. Zhao, Y. Wang and C. Liu, *Food Anal. Methods*, 2022, **15**, 2840–2846.
38 M. Balouiri, M. Sadiki and S. K. Ibnsouda, *J. Pharm. Anal.*, 2015, **6**, 71.
39 T. Schön, J. Werngren, D. Machado, E. Borroni, M. Wijkander, G. Lina, J. Mouton, E. Matuschek, G. Kahlmeter, C. Giske, M. Santin, D. M. Cirillo, M. Viveiros and E. Cambau, *Clin. Microbiol. Infect.*, 2020, **26**, 1488–1492.
40 U. Saleem, M. Saleem, B. Ahmad, K. Hussain, M. Ahmad, N. I. Bukhari, A. A. Anjum and J. Anim, *Plant Sci.*, 2015, **25**(1), 261–267.
41 N. Zhang, X. Li, J. Ye, Y. Yang, Y. Huang, X. Zhang and M. Xiao, *Polymers*, 2020, **12**, 121.

42 Y. Han, L. Zhu, H. Zhang, T. Liu and G. Wu, *Carbohydr. Polym.*, 2024, **339**, 122202.
43 Q. Wen, X. Wang, B. Liu, L. Lu, X. Zhang, C. J. Swing and S. Xia, *Food Biosci.*, 2022, **50**, 102113.
44 N. Kumari, S. P. Bangar, M. Petrů, R. A. Ilyas, A. Singh and P. Kumar, *Foods*, 2021, **10**, 1976.
45 Z. Eslami, S. Elkoun, M. Robert and K. Adjallé, *Molecules*, 2023, **28**, 6637.
46 M. W. Apriliyani, A. Manab, M. W. Apriliyanti and A. D. Ikhwan, *Adv. J. Food Sci. Technol.*, 2020, **18**, 9–14.
47 A. Ajam, Y. Huang, M. S. Islam, K. A. Kilian and J. J. Kruzic, *J. Mech. Behav. Biomed. Mater.*, 2024, **157**, 106642.
48 P. Thivya, N. Bhanu Prakash Reddy, K. Bhosale Yuvraj and V. R. Sinija, *Rev. Environ. Sci. Biotechnol.*, 2023, **22**, 29–53.
49 F. I. S. Amran, A. I. Zamri, H. R. Arifin and A.-H. Shafrina, *J. Biochem. Microbiol. Biotechnol.*, 2024, **12**, 5–8.
50 S. Guzman-Puyol, J. J. Benítez and J. A. Heredia-Guerrero, *Food Res. Int.*, 2022, **161**, 111792.
51 R. Tong, Z. Ma, R. Yao, P. Gu, T. Li, L. Liu, F. Guo, M. Zeng and J. Xu, *Int. J. Biol. Macromol.*, 2023, **246**, 125667.
52 G. Singh, S. Bangar, T. Yang, M. Trif, V. Kumar and D. Kumar, *Polymers*, 2022, **14**, 1987.
53 S. Farooq, S. A. Mir, M. A. Shah, A. Manickavasagan, K. V. Sunooj, M. W. Siddiqui and A. Mousavi Khaneghah, *Starch/Staerke*, 2023, **75**(5–6), 2200098.
54 R. K. Sharme, M. Quijada, M. Terrones and M. M. Rana, *Materials*, 2024, **17**, 4559.
55 X. Li, Y. Liu and X. Ren, *Int. J. Biol. Macromol.*, 2022, **216**, 86–94.
56 C. Wang, S. Tian, Z. Gao, Z. Li, X. An, Y. Lu, Y. Song and Y. Zhao, *J. Food Meas. Charact.*, 2022, **16**, 598–609.
57 K. S. Eça, T. Sartori and F. C. Menegalli, *Braz. J. Food Technol.*, 2014, **17**, 98–112.
58 S. Wang, J. Nan, C. Bi, Y. Gao, B. Mu, J. Wang and C. Liang, *J. Food Prot.*, 2022, **85**, 1027–1035.
59 A. D. Yermagambetova, S. M. Tazhibayeva, B. B. Tyussyupova, K. B. Musabekov and L. Pastorino, *Heliyon*, 2024, **10**, e34550.
60 S. Rahman and D. Chowdhury, *Int. J. Biol. Macromol.*, 2022, **216**, 571–582.
61 A. A. Alshahrani, L. S. Alqarni, M. D. Alghamdi, N. F. Alotaibi, S. M. N. Moustafa and A. M. Nassar, *Heliyon*, 2024, **10**, e24815.
62 H. Ateeq, R. Shabir Ahmad, M. Imran, M. Afzaal and M. Asif Shah, *Int. J. Food Prop.*, 2023, **26**, 2553–2562.
63 H. Rostamabadi, I. Demirkesen, R. Colussi, S. Roy, N. Tabassum, J. G. de Oliveira Filho, Y. Bist, Y. Kumar, M. Nowacka, S. Galus and S. R. Falsafi, *Food Front.*, 2024, **5**, 350–391.
64 T. Cheng, J. Xu, Y. Li, Y. Zhao, Y. Bai, X. Fu, X. Gao and X. Mao, *J. Food Meas. Charact.*, 2021, **15**, 107–118.
65 M. H. Hasan, S. Hossain, M. L. Rahman, G. M. S. Rahman, M. A. Khan and M. A. Al Mamun, *Carbohydr. Polym. Technol. Appl.*, 2025, **10**, 100769.
66 B. Rukmanikrishnan, S. K. Rajasekharan, J. Lee, S. Ramalingam and J. Lee, *Mater. Today Commun.*, 2020, **24**, 101346.
67 H. Carrêlo, A. R. Escoval, P. I. P. Soares, J. P. Borges and M. T. Cidade, *Fluids*, 2022, **7**, 375.
68 B. C. Hancock and G. Zografi, *Pharm. Res.*, 1994, **11**, 471–477.
69 V. Titone, A. Correnti and F. P. La Mantia, *Polymers*, 2021, **13**, 1616.
70 S. Zhang, N. Kim, W. Yokoyama and Y. Kim, *Food Chem.*, 2018, **243**, 202–207.
71 L. Gao, T. Zhu, F. He, Z. Ou, J. Xu and L. Ren, *Coatings*, 2021, **11**, 817.
72 N. A. Sagar and S. Pareek, *Heliyon*, 2020, **6**(11), e05478.
73 K. Dembińska, A. H. Shinde, M. Pejchalová, A. Richert and M. Swiontek Brzezinska, *Foods*, 2025, **14**, 1893.
74 L. Zhao, Y. Zhou, W. Yue, Q. Shen, J. Ke, Y. Ma, L. Zhang and H. Bian, *Food Chem.: X*, 2025, **31**, 103056.
75 Z. Breijyeh, B. Jubeh and R. Karaman, *Molecules*, 2020, **25**, 1340.
76 S. Mardani, M. Moradi, H. Tajik and E. Divsalar, *Int. J. Biol. Macromol.*, 2025, **308**, 142411.
77 M. Kumar, M. D. Barbhai, M. Hasan, S. Dhumal, S. Singh, R. Pandiselvam, N. Rais, S. Natta, M. Senapathy, N. Sinha and R. Amarowicz, *J. Food Sci.*, 2022, **87**, 4289–4311.
78 O.-H. Ali, H. Al-sayed, N. Yasin and E. Afifi, *Bull. Natl. Nutr. Inst.*, 2016, **47**, 1–24.
79 O. T. Beatrice and O. T. Ijsrm, *Int. J. Sci. Res. Methodol.*, 2017, **7**, 25–34.
80 C. Wang, Y. Wang, Y. Song, M. Ren, Z. Gao and J. Ren, *Sci. Rep.*, 2024, **14**, 20816.
81 W. M. Elsherif and A. O. Tolba, *Assiut Vet. Med. J.*, 2024, **70**, 370–385.
82 A. C. Mtibaa, S. Smaoui, H. Ben Hlima, I. Sellem, K. Ennouri and L. Mellouli, *Biomed. Res. Int.*, 2019, **2019**, 1–13.
83 S.-Y. Shim, Y.-S. Choi, H.-Y. Kim, H.-W. Kim, K.-E. Hwang, D.-H. Song, M.-A. Lee, J.-W. Lee and C.-J. Kim, *Food Sci. Biotechnol.*, 2012, **21**, 565–572.
84 A. U. Alahakoon, Y. S. Bae, H. J. Kim, S. Jung, D. D. Jayasena, H. I. Yong, S. H. Kim and C. Jo, *Korean J. Agric. Sci.*, 2013, **40**, 131–137.
85 T.-H.-A. Phan, T.-P. Nguyen and T.-T.-A. Tran, *IOP Conf. Ser.: Earth Environ. Sci.*, 2021, **947**, 012042.
86 N. A. Sagar and S. Pareek, *Food Biosci.*, 2021, **41**, 100992.
87 W. M. Umeda and N. Jorge, *Food Control*, 2021, **127**, 108130.
88 Ł. J. Walczak-Nowicka and M. Herbet, *Nutrients*, 2022, **14**, 1497.